

# Perturbative QCD analysis of Dalitz decays $J/\psi \rightarrow \eta^{(\prime)} \ell^+ \ell^-$

Jun-Kang He\* and Chao-Jie Fan†

*Institute of Particle Physics and Key Laboratory of Quark and Lepton Physics (MOE),  
Central China Normal University, Wuhan, Hubei 430079, P. R. China*

In the framework of perturbative QCD, we study the Dalitz decays  $J/\psi \rightarrow \eta^{(\prime)} e^+ e^-$  with large recoil momentum. Meanwhile, the soft contributions from the small recoil momentum region and the VMD corrections have also been taken into account. The transition form factors  $f_{\psi\eta^{(\prime)}}(q^2)$  including the hard and soft contributions as well as the VMD corrections are calculated for the first time. By analytical evaluation of the involved one-loop integrals, we find that the transition form factors are insensitive to both the light quark masses and the shapes of  $\eta^{(\prime)}$  distribution amplitudes. With the normalized transition form factors, our results of the branching ratios  $\mathcal{B}(J/\psi \rightarrow \eta^{(\prime)} e^+ e^-)$  and their ratio  $R_{J/\psi}^e = \mathcal{B}(J/\psi \rightarrow \eta e^+ e^-)/\mathcal{B}(J/\psi \rightarrow \eta' e^+ e^-)$  are in good agreement with their experimental data. Furthermore, by the ratio  $R_{J/\psi}^e$ , we extract the mixing angle of  $\eta - \eta'$  system  $\phi = 34.0^\circ \pm 0.6^\circ$  and comment on this result briefly. Inputting the mixing angle  $\phi$  extracted from  $R_{J/\psi}^e$ , we predict the branching ratios  $\mathcal{B}(J/\psi \rightarrow \eta \mu^+ \mu^-) = 3.64 \times 10^{-6}$ ,  $\mathcal{B}(J/\psi \rightarrow \eta' \mu^+ \mu^-) = 1.52 \times 10^{-5}$  and their ratio  $R_{J/\psi}^\mu = 23.9\%$ .

## I. INTRODUCTION

The decays of charmonia into light hadrons have received a great deal of attention in the past few decades both experimentally and theoretically, since they provide us with invaluable information on quantum chromodynamics (QCD) strong interactions between quarks and gluons. In the QCD picture, the decays of charmonia into light hadrons are expected to proceed predominantly via  $c\bar{c}$  annihilation with an intermediate state containing only gluons, so they are ideal for the study of light hadron production mechanisms and the involved dynamical information can be extracted. In recent years, several groups have revisited the radiative decays  $J = \psi \rightarrow \eta^{(\prime)}$  [1–6] as well as  $h_c \rightarrow \eta^{(\prime)}$  [7] in the framework of perturbative QCD (pQCD), since these decay processes are related to the issue of  $\eta - \eta'$  mixing from which the mixing angle and the decay constants  $f_{q(s)}$  can be extracted [2, 6, 7]. Furthermore, these investigations show that the pQCD approach is still useful for our understanding of the charmonium physics.

Recently, the BESIII Collaboration has updated the measurements of the electromagnetic (EM) Dalitz decays  $J = \psi \rightarrow \eta^{(\prime)} e^+ e^-$  with the branching ratios  $\mathcal{B}(J = \psi \rightarrow \eta e^+ e^-) = (1.43 \pm 0.04 \pm 0.06) \times 10^{-5}$  [8] and  $\mathcal{B}(J = \psi \rightarrow \eta' e^+ e^-) = (6.59 \pm 0.07 \pm 0.17) \times 10^{-5}$  [9]. As the EM Dalitz decays of light vector mesons ( $\rho^0, \omega, \phi$ ), which have attracted much attention in both experiment [10–15] and theory [16–21], these decay processes also provide a clean environment to study the dynamical structure of the transition form factors (TFFs)  $f_{VP}(q^2)$  and offer a potential role in the theoretical determination of the hypothetical dark photon (i.e., the U-boson) [8, 9, 17, 22]. In addition, the Dalitz decays  $J = \psi \rightarrow \eta^{(\prime)} \ell^+ \ell^-$  ( $\ell = e, \mu$ ) are especially interesting since they involve the production of the light mesons  $\eta^{(\prime)}$ , which are of great phenomenological importance because of  $\eta - \eta'$  mixing effects.

In the literature, the Dalitz decays  $J = \psi \rightarrow \eta^{(\prime)} \ell^+ \ell^-$  have been studied in different approaches [22–24]. In works [22, 24], the normalized TFFs  $F_{\psi\eta^{(\prime)}}(q^2)$  were parameterized as a simple pole form and the branching ratios of  $J = \psi \rightarrow \eta^{(\prime)} \ell^+ \ell^-$  were calculated with the vector meson dominance (VMD) model. Although their predictions of the branching ratios  $\mathcal{B}(J = \psi \rightarrow \eta^{(\prime)} e^+ e^-)$  are compatible with the experimental measurements [8, 9], the normalized TFFs  $F_{\psi\eta^{(\prime)}}(q^2)$ , which are defined as  $F_{\psi\eta^{(\prime)}}(q^2) \equiv f_{\psi\eta^{(\prime)}}(q^2)/f_{\psi\eta^{(\prime)}}(0)$  in their papers [22, 24], would gloss over the dynamical information from the QCD processes where the dynamical information will offer us an insight into the nature of the Okubo-Zweig-Iizuka (OZI) rule [25, 26] and the  $U_A(1)$  anomaly as well as the  $\eta - \eta'$  mixing [2, 6, 27–30]. Therefore, a good theoretical study of the TFFs  $f_{\psi\eta^{(\prime)}}(q^2)$  (or, the normalized TFFs  $F_{\psi\eta^{(\prime)}}(q^2)$ ) should include the dynamical information of the mesons' structure. We will present detailed discussions in a later part. Besides the phenomenological model, Chen *et al.* [23] studied these Dalitz decay processes with the effective Lagrangian approach, and they confirmed that the  $J = \psi \rightarrow \eta^{(\prime)} \ell^+ \ell^-$  processes were predominantly dominated by the  $J = \psi \rightarrow c \bar{c} \rightarrow \eta^{(\prime)} \ell^+ \ell^-$  mechanism. Perhaps this may be less reliable [6].

In principle, there are several types of contributions to the TFFs involved in the EM Dalitz decay processes  $J = \psi \rightarrow \eta^{(\prime)} \ell^+ \ell^-$ : (i) In the large recoil momentum region,  $q^2 \simeq 0$ , the contributions are dominated by the hard mechanism, which can be calculated in the framework of pQCD. Just as our recent investigations [6, 7], the pQCD approach can be well employed in the radiative decay processes  $J = \psi (h_c) \rightarrow \eta^{(\prime)}$ . (ii) In the small recoil momentum region,  $q^2 \simeq q_{\text{max}}^2$ , phenomenologically, the TFFs can be interpreted as the wave function overlap [31]. Namely, the corresponding contributions (i.e., soft contributions) are

\* Electronic address: [hejk@mails.cnu.edu.cn](mailto:hejk@mails.cnu.edu.cn)

† Corresponding author: [fancj@mails.cnu.edu.cn](mailto:fancj@mails.cnu.edu.cn)

governed by the overlap of their wave functions. (iii) In some resonance regions, such as  $q^2 \simeq m_\rho^2; m_\omega^2; m_\phi^2$ , the resonance interaction between photons and hadrons is predominant, which can be universally described by a vector meson dominance (VMD) model [16]. It is worth noting that this mechanism provides only small corrections to the branching ratios  $\mathcal{B}(J = \rightarrow (\ell^+ \ell^-))$  in the whole region due to the suppression of the kinematic factors, and more details can be found in the later sections. In this work, we include the contributions from the hard mechanism and the soft wave function overlap to study these Dalitz decay processes  $J = \rightarrow (\ell^+ \ell^-)$ . In addition, we also comment the contributions from VMD. It should be pointed out that the radiative corrections are also important in the case of electron pair production. However, a full analysis of radiative corrections seems highly impractical since it would require a two-loop calculation. Of course, the radiative corrections are negligibly small in the case of muon pair production [16].

In this paper, a detailed perturbative QCD analysis of the Dalitz decays  $J = \rightarrow (\ell^+ \ell^-)$  are presented. In the large recoil momentum region, we evaluate analytically the involved one-loop integrals, and find the TFFs barely depend on the light quark masses and the shapes of the light meson distribution amplitudes (DAs), which is compatible with the situation in the decay processes  $J = \rightarrow (\ell^+ \ell^-)$  [6] as well as  $h_c \rightarrow (\ell^+ \ell^-)$  [7]. Considering the contributions from the hard and soft processes as well as the VMD corrections, our result of the normalized TFF  $F_{\psi\eta}(q^2)$  is in good agreement with the experimental data. By using the phenomenological parameters of  $\eta - \eta'$  mixing extracted from the decay processes  $J = \rightarrow (\ell^+ \ell^-)$ , we obtain the predictions of the branching ratios  $\mathcal{B}(J = \rightarrow (\ell^+ \ell^-))$  and their ratio  $\mathcal{R}_{J/\psi}^\mu$ .

The paper is organized as follows. The theoretical framework for the decay processes  $J = \rightarrow (\ell^+ \ell^-)$  is presented in section II. In section III we present our numerical results and some phenomenological discussions while section IV is our summary.

## II. THEORETICAL FRAMEWORK

### A. Hard mechanism

#### 1. The contributions of the quark-antiquark content of $\eta^{(\prime)}$

For the quark-antiquark content of  $\eta^{(\prime)}$ , one of the leading order Feynman diagrams for the decay processes  $J = \rightarrow (\ell^+ \ell^-)$  is depicted in Fig. 1, and the other five diagrams arise from permutations of the photon and gluon legs. According to the Feynman diagrams, we can easily give the amplitude of  $J = \rightarrow (\ell^+ \ell^-)$ :

$$\mathcal{M} = -\frac{e}{q^2} \mathcal{A}^{\alpha\beta\mu\nu}{}_{\alpha}(\mathbf{K}) \bar{u}(l_1) \gamma_\mu v(l_2); \quad (1)$$

where  $\mathcal{A}$  (i.e.,  $\mathcal{A}^{\alpha\beta\mu\nu}{}_{\alpha}(\mathbf{K}) \gamma_\beta(q)$ ) is the amplitude of  $J = \rightarrow (\ell^+ \ell^-)$ ,  $\mathbf{K}$  and  $\mu(\mathbf{K})$  are the momentum and polarization vector of  $J =$  respectively,  $q$  is the momentum of the virtual photon,  $q^2 = m_{\ell^+ \ell^-}^2$  is the effective mass squared of the lepton pair,  $l_1$  and  $l_2$  are the momenta of the leptons  $\ell^-$  and  $\ell^+$  respectively.

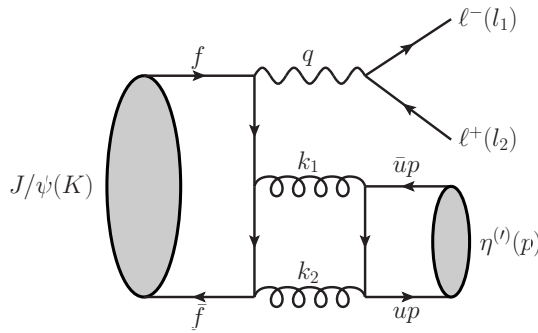


FIG. 1. One typical Feynman diagram for  $J/\psi \rightarrow \eta^{(\prime)} \ell^+ \ell^-$  with the quark-antiquark content of  $\eta^{(\prime)}$ . The kinematical variables are labeled.

Following the method developed in Refs. [32–34], we divide the amplitude of  $J = \rightarrow (\ell^+ \ell^-)$  into two parts. One part describes the effective coupling between  $J =$ , a virtual photon and two virtual gluons, i.e., the process  $J = \rightarrow g^* g^*$ . The other part describes the effective coupling between  $\eta^{(\prime)}$  and two virtual gluons, i.e., the processes  $g^* g^* \rightarrow \eta^{(\prime)}$ . Then we just multiply the two parts, insert the gluon propagators and perform the loop integrations to obtain the final amplitude of  $J = \rightarrow (\ell^+ \ell^-)$ .

In the rest frame of  $J =$ , one can write the amplitude of  $J = \rightarrow g^* g^*$  in the form [33–35]

$$\mathcal{A}_1^{\alpha\beta\mu\nu}{}_{\alpha}(\mathbf{K}) \gamma_\beta(q) \gamma_\mu(k_1) \gamma_\nu(k_2) = \sqrt{3} \int \frac{d^4k}{(2\pi)^4} \text{Tr} [ (\mathbf{K}; k) \mathcal{O}(k) ]; \quad (2)$$

where  $\mathcal{K}(K; k)$  is the Bethe-Salpeter (B-S) wave function of  $J = 1^-$  and  $\mathcal{O}(k)$  is the hard-scattering amplitude. Here  $\sqrt{3}$  is the color factor and  $\mathcal{Q}$  is the polarization vector of the virtual photon.  $k_1, k_2$  and  $\mathcal{Q}(k_1), \mathcal{Q}(k_2)$  are the momenta and polarization vectors of the two gluons, respectively. The momenta of the quark  $c$  and antiquark  $\bar{c}$  read

$$\mathbf{f} = \frac{\mathbf{K}}{2} + \mathbf{k}; \quad \bar{\mathbf{f}} = \frac{\mathbf{K}}{2} - \mathbf{k} \quad (3)$$

with  $k$  the relative momentum between the quark  $c$  and antiquark  $\bar{c}$ . In a nonrelativistic bound state picture, one can reduce the B-S wave function  $\mathcal{K}(K; k)$  to its nonrelativistic form [32, 35]

$$\mathcal{K}(K; k) = 2 \mathcal{R}(k^0) \mathcal{R}_{00}(\mathbf{k}) \left[ \sqrt{\frac{1}{4M}} \mathcal{O}(\mathbf{K})(\mathbf{K} - M) \right]; \quad (4)$$

where  $\mathcal{R}_{00}(\mathbf{k})$  is the bound state wave function of S-wave charmonium  $J = 1^-$ . We may neglect the dependence of the hard-scattering amplitude  $\mathcal{O}(k)$  on the relative momentum  $k$  in the leading order approximation [6, 35, 36]:

$$\mathcal{O}(k) \simeq \mathcal{O}(0); \quad (5)$$

because the B-S wave function  $\mathcal{K}(K; k)$  is heavily damped on the relative momentum. Using the Fourier transformation of the bound state wave function

$$\int \frac{d^3k}{(2\pi)^3} \mathcal{R}_{00}(\mathbf{k}) = \sqrt{\frac{1}{4}} \mathcal{R}_\psi(0); \quad (6)$$

we obtain the well-known result in coordinate space. With the help of the B-S wave function Eq. (4) and the hard-scattering amplitude Eq. (5) as well as the Fourier transformation Eq. (6), the amplitude of  $J = 1^- \rightarrow g^* g^*$  can be rewritten as

$$\mathcal{A}_1^{\alpha\beta\mu\nu} \mathcal{O}_\alpha(K) \mathcal{Q}_\beta(q) \mathcal{Q}_\mu(k_1) \mathcal{Q}_\nu(k_2) = \frac{1}{2} \sqrt{\frac{3}{4M}} \mathcal{R}_\psi(0) \text{Tr} \left[ \mathcal{O}(K)(\mathbf{K} - M) \mathcal{O}(0) \right]; \quad (7)$$

where the hard-scattering amplitude  $\mathcal{O}(0)$  reads

$$\mathcal{O}(0) = i Q_c e g_s^2 \frac{ab}{6} \mathcal{Q}_\alpha(k_2) \frac{\mathbf{k}_2 - \mathbf{q} - \mathbf{k}_1 + M}{-2(\mathbf{q} + \mathbf{k}_1) \cdot \mathbf{k}_2} \mathcal{Q}_\beta(q) \frac{\mathbf{k}_2 + \mathbf{q} - \mathbf{k}_1 + M}{-2(\mathbf{q} + \mathbf{k}_2) \cdot \mathbf{k}_1} \mathcal{Q}_\mu(k_1) + (5 \text{ permutations of } k_1, k_2 \text{ and } q); \quad (8)$$

What follows is a brief summary of the processes  $g^* g^* \rightarrow \mathcal{V}^{(\prime)}$ . At the leading twist level, the light-cone DA of the meson  $\mathcal{V}^{(\prime)}$  is defined according to [37–39]

$$\langle \mathcal{V}^{(\prime)}(\mathbf{p}) | \bar{q}_\alpha(x) q_\beta(y) | 0 \rangle = \frac{i}{4} f_{\eta^{(\prime)}}^q (\mathbf{p} \cdot \mathbf{5})_{\beta\alpha} \int du e^{i(\bar{u}p \cdot y + up \cdot x)} q(u); \quad (9)$$

where the superscript  $q$  denotes the light quark ( $q = u; d; s$ ) and  $\mathbf{p}$  represents the momentum of  $\mathcal{V}^{(\prime)}$ . The decay constants  $f_{\eta^{(\prime)}}^q$  are defined according to

$$\langle 0 | \bar{q}(0) \gamma_\mu \mathbf{5} q(0) | \mathcal{V}^{(\prime)}(\mathbf{p}) \rangle = i f_{\eta^{(\prime)}}^q \mathbf{p}_\mu; \quad (10)$$

Using the light-cone matrix elements of the quark-antiquark content of  $\mathcal{V}^{(\prime)}$  Eq. (9), we obtain the amplitude of  $g^* g^* \rightarrow \mathcal{V}^{(\prime)}$  [40–42]:

$$\mathcal{A}_2^{\mu\nu} = -i(4 - s)_{ab} \mu^{\nu\rho\sigma} k_{1\rho} k_{2\sigma} \sum_{q=u,d,s} \frac{f_{\eta^{(\prime)}}^q}{6} \int_0^1 du q(u) \left( \frac{1}{\bar{u}k_1^2 + uk_2^2 - u\bar{u}m^2 - m_q^2} + (u \leftrightarrow \bar{u}) \right); \quad (11)$$

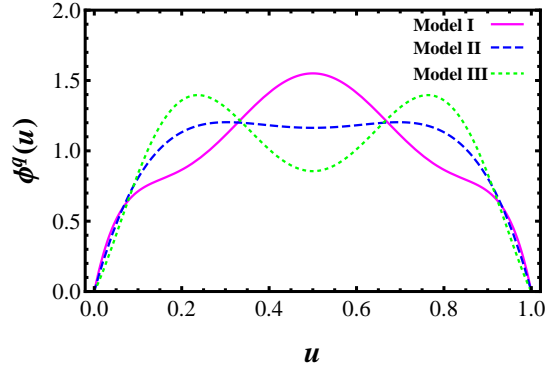
Here  $\bar{u} = 1 - u$ ,  $u$  is the momentum fraction carried by the quark,  $m_q$  is the mass of the quark ( $q = u; d; s$ ),  $m$  is the mass of  $\mathcal{V}^{(\prime)}$ . The light-cone DA is [43]

$$q(u) = 6u(1-u) \left[ 1 + \sum_{n=2,4,\dots} c_n^q \langle \mathcal{V}^{(\prime)} | C_n^{\frac{3}{2}}(2u-1) \right] \quad (12)$$

with  $c_n^q(\mathcal{V}^{(\prime)})$  the Gegenbauer moments. In table I, we list three models of the DAs discussed in Ref. [43]. Schematically, we also show their shapes in Fig. 2.

TABLE I. Gegenbauer coefficients of three sample models at the scale  $\mu_0 = 1$  GeV.

Model	$c_2^a(\mu_0)$	$c_4^a(\mu_0)$	$c_2^g(\mu_0)$
I	0.10	0.10	-0.26
II	0.20	0.00	-0.31
III	0.25	-0.10	-0.25

FIG. 2. The shapes of the corresponding DAs with the scale  $\mu = M/2$ .

Then the final decay amplitude of  $J = \rightarrow (\prime) *$  can be obtained by contracting the above two couplings, inserting the gluon propagators and integrating over the loop momentum (see [33, 34] for more details)

$$\mathcal{A} = \mathcal{A}^{\alpha\beta} \alpha_{\alpha}(\mathbf{K}) \beta_{\beta}(\mathbf{q}) = \frac{1}{2} \int \frac{d^4 k_1}{(2\pi)^4} \mathcal{A}_1^{\alpha\beta\mu\nu} \mathcal{A}_{2\mu\nu} \frac{i}{k_1^2 + i} \frac{i}{k_2^2 + i} \alpha_{\alpha}(\mathbf{K}) \beta_{\beta}(\mathbf{q}); \quad (13)$$

i.e.,

$$\mathcal{A}^{\alpha\beta} = \frac{1}{2} \int \frac{d^4 k_1}{(2\pi)^4} \mathcal{A}_1^{\alpha\beta\mu\nu} \mathcal{A}_{2\mu\nu} \frac{i}{k_1^2 + i} \frac{i}{k_2^2 + i}; \quad (14)$$

Considering parity conservation, Lorentz invariance and gauge invariance, we know that

$$\mathcal{A}^{\alpha\beta} \propto (\alpha^{\beta\mu\nu} p_{\mu} q_{\nu}); \quad (15)$$

To proceed, we can define the  $J = \rightarrow (\prime) *$  TFF according to

$$\mathcal{A}^{\alpha\beta} = -e f_{\psi\eta}^Q(q^2) \alpha^{\beta\mu\nu} p_{\mu} q_{\nu}; \quad (16)$$

With the help of a projection operator

$$\mathcal{P}^{\alpha\beta} = \frac{\alpha^{\beta\mu\nu} p_{\mu} q_{\nu}}{\frac{1}{2}(M^2; m^2; q^2)} \quad (17)$$

and the normalization condition

$$\mathcal{P}^{\alpha\beta} \mathcal{P}_{\alpha\beta} = \frac{1}{2}; \quad (18)$$

the TFF can be rewritten as

$$f_{\psi\eta}^Q(q^2) = -\frac{2e^{-1}}{\frac{1}{2}(M^2; m^2; q^2)} \mathcal{P}_{\alpha\beta} \mathcal{A}^{\alpha\beta} \quad (19)$$

with  $(a; b; c) \equiv a^2 + b^2 + c^2 - 2(ab + bc + ac)$  the usual Källén function. Substituting  $\mathcal{A}^{\alpha\beta}$  given in Eq. (14) into Eq. (19), we obtain

$$f_{\psi\eta}^Q(q^2) = \frac{e^{-1}}{\frac{1}{2}(M^2; m^2; q^2)} \int \frac{d^4 k_1}{(2\pi)^4} \mathcal{A}_1^{\alpha\beta\mu\nu} \mathcal{A}_{2\mu\nu} \mathcal{P}_{\alpha\beta} \frac{1}{k_1^2 + i} \frac{1}{k_2^2 + i}; \quad (20)$$

Here we show the analytical expression of the TFF more clearly

$$\begin{aligned}
f_{\psi\eta^{(\prime)}}^Q(q^2) &= \frac{16R_\psi(0)}{(M^2; m^2; q^2)} \frac{Q_c(4s)^2}{3\sqrt{3}} \sqrt{\frac{M}{-}} \sum_q f_{\eta^{(\prime)}}^q \int du^q(u) \int \frac{d^4k_1}{(2\pi)^4} \frac{(k_1^2 - k_1 \cdot p)}{(M^2 - m^2 - q^2)} \\
&\times \left[ \frac{(k_1 \cdot p (M^2 - m^2 - q^2) (4k_1 \cdot q + M^2 - m^2 - q^2) - 2m^2 k_1 \cdot q (M^2 - m^2 - q^2) - 8q^2 k_1 \cdot p^2}{2D_1 D_2 D_3 D_4 D_5} \right. \\
&\quad \left. - \frac{(M^2; m^2; q^2)}{D_2 D_3 D_4 D_5} \right) + (u \leftrightarrow \bar{u}) \Big]; \tag{21}
\end{aligned}$$

where the expressions of the denominators read

$$\begin{aligned}
D_1 &= k_1^2 + i \\
D_2 &= (k_1 - p)^2 + i \\
D_3 &= (k_1 - up)^2 - m_q^2 + i \\
D_4 &= \frac{1}{4} [(2k_1 - p - q)^2 - M^2] + i \\
D_5 &= \frac{1}{4} [(2k_1 - p + q)^2 - M^2] + i : \tag{22}
\end{aligned}$$

By using the algebraic identity

$$1 = \frac{2(D_1 + D_2 - D_4 - D_5)}{M^2 + m^2 - q^2}; \tag{23}$$

the TFF  $f_{\psi\eta^{(\prime)}}^Q(q^2)$  in Eq. (21) can be decomposed into sum of four-point one-loop integrals, and then it can be analytically evaluated with the technique proposed in Refs. [44–46] or the computer program Package-X [47, 48]. By integrating over the loop momentum  $k_1$  and the momentum fraction  $u$ , we find that the TFF  $f_{\psi\eta^{(\prime)}}^Q(q^2)$  is very insensitive to the light quark mass  $m_q$  as well as the shapes of  $\eta^{(\prime)}$  DAs. This is similar to the situations of the dimensionless functions involved in the radiative decays  $J = (\eta_c) \rightarrow \eta^{(\prime)}$  [6, 7]. Specifically, the change of the modulus of the TFF  $f_{\psi\eta^{(\prime)}}^Q(q^2)$  does not exceed 1% when the value of the light quark mass  $m_q$  varies in the range 0–100 MeV for all the three kinds of  $\eta^{(\prime)}$  DAs in Fig. 2. So in the following numerical calculations, we choose the Model I in Table I for the DA with the scale  $\mu = M=2$ .

It is worthwhile to point out that the QED processes  $J = \eta_c \rightarrow \eta^{(\prime)} \ell^+ \ell^-$  can also contribute to the EM Dalitz decays  $J = \eta_c \rightarrow \eta^{(\prime)} \ell^+ \ell^-$  and the corresponding Feynman diagrams are shown in Fig. 3. Then the corresponding TFF  $f_{\psi\eta^{(\prime)}}^E(q^2)$  can be

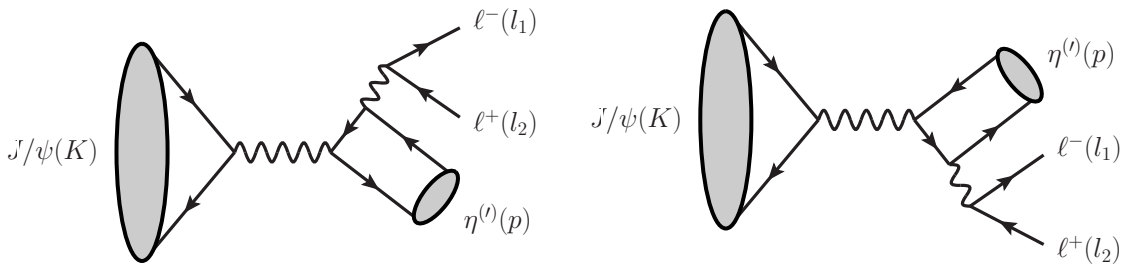


FIG. 3. Feynman diagrams for the QED processes  $J/\psi \rightarrow \gamma^* \rightarrow \eta^{(\prime)} \ell^+ \ell^-$ . The kinematical variables are labeled.

expressed as

$$\begin{aligned}
f_{\psi\eta^{(\prime)}}^E(q^2) &= i\sqrt{3}Q_c(4s) \frac{R_\psi(0)}{M^2} \sqrt{\frac{M}{-}} \sum_{q=u,d,s} Q_q^2 f_{\eta^{(\prime)}}^q \int du^q(u) \\
&\times \left[ \frac{1}{q^2 + u^2 m^2 + u(M^2 - m^2 - q^2) - m_q^2 + i} + (u \leftrightarrow \bar{u}) \right]; \tag{24}
\end{aligned}$$

where the  $Q_q$  represents the light quark charge.

## 2. The contributions of the gluonic content of $\eta^{(\prime)}$

As we have emphasized in Ref. [6], the contributions of the gluonic content of  $\eta^{(\prime)}$  in the radiative decay processes  $J = \eta^{(\prime)} \rightarrow \ell^+ \ell^-$  can directly come from the tree level and the amplitude is strongly suppressed by the factor  $m^2 = M^2$ . Obviously, the situation should be found in the Dalitz decay processes  $J = \eta^{(\prime)} \rightarrow \ell^+ \ell^- \gamma$ , because the Dalitz decay processes and the corresponding radiative decay processes have the same spin structures in their amplitudes. The typical Feynman diagram is exhibited in Fig. 4, and there are the other two diagrams from permutations of the photon and gluon legs.

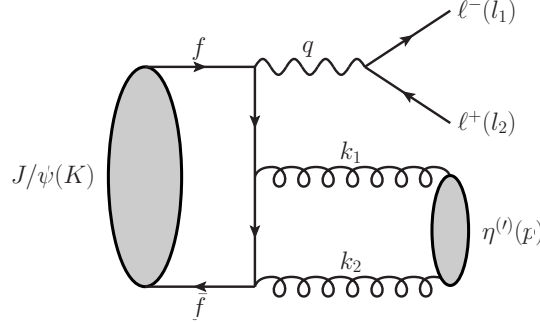


FIG. 4. One typical Feynman diagram for  $J/\psi \rightarrow \eta^{(\prime)} \ell^+ \ell^-$  with the gluonic content of  $\eta^{(\prime)}$ . The kinematical variables are labeled.

At the leading twist level, the light-cone matrix elements of the meson  $\eta^{(\prime)}$  over two-gluon fields can be written as [39, 43, 49]:

$$\langle \eta^{(\prime)}(p) | A_\alpha^a(x) A_\beta^b(y) | 0 \rangle = \frac{1}{4} \frac{\epsilon^{\mu\nu\alpha\beta} n^\mu p^\nu C_F}{p \cdot n \sqrt{3}} \frac{ab}{8} f_{\eta^{(\prime)}}^1 \int du e^{i(up \cdot x + \bar{u}p \cdot y)} \frac{g(u)}{u(1-u)}; \quad (25)$$

where  $n = (0; 1; \mathbf{0}_\perp)$  is a lightlike vector [49]. Here  $f_{\eta^{(\prime)}}^1 = \frac{1}{\sqrt{3}}(f_{\eta^{(\prime)}}^u + f_{\eta^{(\prime)}}^d + f_{\eta^{(\prime)}}^s)$  is the effective decay constant and the gluonic twist-2 DA reads [39, 43, 50]

$$g(u) = 30u^2(1-u)^2 \sum_{n=2,4,\dots} c_n^g(\eta^{(\prime)}) C_{n-1}^{\frac{5}{2}}(2u-1); \quad (26)$$

After a series of calculations, the corresponding TFF  $f_{\psi\eta^{(\prime)}}^G(q^2)$  can be expressed as

$$f_{\psi\eta^{(\prime)}}^G(q^2) = i \frac{8R_\psi(0)}{(M^2; m^2; q^2)} \frac{Q_c(4s)}{9} \sqrt{M} f_{\eta^{(\prime)}}^1 \int du \frac{g(u)}{u(1-u)} \frac{m^2(M^2 - m^2 - q^2)(1-2u)}{[(M^2 - q^2)^2 - m^4(1-2u)^2]}. \quad (27)$$

Clearly, there is a suppression factor of  $m^2$  (or, a dimensionless factor  $m^2 = M^2$ ) in the TFF  $f_{\psi\eta^{(\prime)}}^G(q^2)$  of Eq. (27). As pointed out in Ref. [6], the leading twist gluonic content contributions are almost two on-shell gluons contributions, which are suppressed by the factor  $m^2 = M^2$  due to the special form of the Ore-Powell matrix elements as found in Refs. [51, 52] years ago. In addition, the contributions from the gluonic content of  $\eta^{(\prime)}$  are supposed to be small since the gluonic content can be seen as the higher-order effects from the point of view of the QCD evolution of the gluon DA.

Based on the foregoing discussion, in the large recoil momentum region, the  $J = \eta^{(\prime)} \rightarrow \ell^+ \ell^- \gamma$  TFF can be obtained by

$$f_{\psi\eta^{(\prime)}}^H(q^2) = f_{\psi\eta^{(\prime)}}^Q(q^2) + f_{\psi\eta^{(\prime)}}^E(q^2) + f_{\psi\eta^{(\prime)}}^G(q^2); \quad (28)$$

which includes the dynamical information from the QCD and QED processes. And all these contributions can be calculated in the framework of pQCD.

### B. Soft mechanism

In the small recoil momentum region, the pQCD approach becomes invalid in the EM Dalitz decay processes  $J = \eta^{(\prime)} \rightarrow \ell^+ \ell^- \gamma$ . And the dominant contributions to the  $J = \eta^{(\prime)} \rightarrow \ell^+ \ell^- \gamma$  TFF come from the soft mechanism, which can be treated as the soft wave function overlap. phenomenologically, we can adopt an empirical form factor [31, 53]:

$$f_{\psi\eta^{(\prime)}}^S(q^2) = g_{\psi\eta^{(\prime)}} \exp\left(-\frac{q^2}{8}\right); \quad (29)$$

where  $g_{\psi\eta^{(\prime)}}$  denotes the  $J = \eta^{(\prime)}$  coupling and is determined by the continuity condition of the TFF between the large and small recoil momentum regions, and the parameter  $M$  is in a range of 300 – 500 MeV [31, 53]. Our numerical analysis indicates that a large value of  $M = 450$  MeV is favored, since some part of the hard contributions, which come from the hard processes by the continuity condition, would be absorbed into the parameter  $g_{\psi\eta^{(\prime)}}$ .

So, in the whole recoil momentum region, the  $J = \eta^{(\prime)}$  TFF can be expressed as

$$f_{\psi\eta^{(\prime)}}(q^2) = \begin{cases} f_{\psi\eta^{(\prime)}}^H(q^2) & q^2 \leq 1 \text{ GeV}^2; \\ f_{\psi\eta^{(\prime)}}^S(q^2) & q^2 > 1 \text{ GeV}^2; \end{cases} \quad (30)$$

Although we can clearly separate the hard contributions in the large recoil momentum region and the soft contributions in the small recoil momentum region, how to match these two contributions at intermediate recoil is an open problem. Even so, our description of the  $J = \eta^{(\prime)}$  TFF may constitute an important step forward towards a satisfactory description.

### C. VMD model

In this subsection we will briefly discuss the resonance interaction, which can be described by a VMD model. The VMD contributing diagram is illustrated in Fig. 5, in which the vector meson  $V$  includes the light mesons  $\rho$ ,  $\omega$  and  $\phi$ .

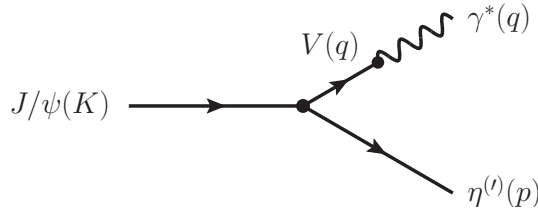


FIG. 5. Schematic diagram for  $J/\psi \rightarrow \eta^{(\prime)}\gamma^*$  in the frame of VMD. The kinematical variables are labeled.

Lagrangian for  $J = \eta^{(\prime)} - V - P$  coupling can be written as [31, 53–55]:

$$\mathcal{L}_{\psi VP} = \frac{g_{\psi VP}(q^2)}{M} \alpha_{\beta\mu\nu} \partial^\alpha \beta_{\alpha\mu} V^\nu P; \quad (31)$$

where  $V^\nu$  ( $V = \rho; \omega; \phi$ ),  $\beta_{\alpha\mu}$  ( $\beta = J = \eta^{(\prime)}$ ) and  $P$  ( $P = \eta^{(\prime)}$ ) are the corresponding vector and pseudoscalar meson fields,  $g_{\psi VP}(q^2) = g_{\psi VP} \exp\left(\frac{-q^2}{8\beta^2}\right)$  is dimensionless coupling constant (see Refs. [31, 53] for more details) and the undetermined constant  $g_{\psi VP}$  can be determined by the decay process  $J = \eta^{(\prime)} \rightarrow VP$ . Following the effective Lagrangian of Eq (31), one can easily derive the undetermined constant:

$$g_{\psi VP} = \left( \frac{96 M^5 \Gamma_{J/\psi \rightarrow V \eta^{(\prime)}}^{exp}}{\frac{3}{2} (M^2; m_V^2; m^2)} \right)^{\frac{1}{2}} \exp\left( \frac{(M^2; m_V^2; m^2)}{32M^2} \right); \quad (32)$$

where  $m_V$  is the mass of the vector meson  $V$ . And the effective Lagrangian for  $V - \gamma^*$  coupling can be described as [31, 53, 56]:

$$\mathcal{L}_{V\gamma^*} = \frac{em_V^2}{f_V} V_\mu A^\mu; \quad (33)$$

where  $em_V^2 = f_V$  is the photon-vector-meson coupling constant,  $A^\mu$  denotes the EM field. The undetermined constant  $f_V$  can be extracted from the decay process  $V \rightarrow e^+e^-$ :

$$|f_V| = \left( \frac{4 m_V^2}{3 \Gamma_{V \rightarrow e^+e^-}^{exp}} \right)^{\frac{1}{2}}; \quad (34)$$

Then the corresponding TFF can be read as

$$f_{\psi\eta^{(\prime)}}^V(q^2) = -i \frac{g_{\psi VP}(q^2) m_V^2}{M f_V (q^2 - m_V^2 + im_V \Gamma_V)}; \quad (35)$$

where  $\Gamma_V$  is the full width of the vector meson  $V$ . When the intermediate vector meson is near the on-mass-shell, we have

$$\mathbf{f}_{\psi\eta^{(\prime)}}^V \sim \left( \frac{\Gamma_{J/\psi \rightarrow V\eta^{(\prime)}}^{exp}}{\Gamma_V} \right)^{\frac{1}{2}} \mathcal{B}^{exp}(V \rightarrow e^+e^-)^{\frac{1}{2}}; \quad (36)$$

which means that the TFFs  $\mathbf{f}_{\psi\eta^{(\prime)}}^\rho$  are an order of magnitude smaller than the TFFs  $\mathbf{f}_{\psi\eta^{(\prime)}}^{\omega,\phi}$  due to the smaller decay widths  $\Gamma_{J/\psi \rightarrow \rho\eta^{(\prime)}}^{exp}$  and branching ratio  $\mathcal{B}^{exp}(V \rightarrow e^+e^-)$  as well as the larger full width  $\Gamma_\rho$  [57]. It is worth noting that there is still some open questions, such as the sign ambiguity in the generalized amplitude from the intermediate vector mesons ( $\rho$ ;  $\omega$ ;  $\phi$ ) and the off-mass-shell effects of the coupling constants, and more discussions could be found in Ref. [54].

### III. RESULTS AND DISCUSSIONS

The  $q^2$ -dependent differential decay widths of  $J = \rightarrow (\prime)^{+\prime-}$  can be expressed as

$$\frac{d\Gamma(J = \rightarrow (\prime)^{+\prime-})}{dq^2} = \frac{1}{3} \frac{2}{24} \frac{1}{M^3} \frac{|\mathbf{f}_{\psi\eta^{(\prime)}}(q^2)|^2}{q^2} \left(1 + \frac{2m_\ell^2}{q^2}\right) \left(1 - \frac{4m_\ell^2}{q^2}\right)^{\frac{1}{2}} \frac{3}{2} (M^2; m^2; q^2); \quad (37)$$

where  $m_\ell$  is the lepton mass. In order to remove most part of the uncertainties from the TFF  $\mathbf{f}_{\psi\eta^{(\prime)}}(q^2)$ , we relate the differential decay widths  $d\Gamma(J = \rightarrow (\prime)^{+\prime-})$  to the corresponding radiative decay widths  $\Gamma(J = \rightarrow (\prime)^{+\prime-})$ :

$$\frac{d\Gamma(J = \rightarrow (\prime)^{+\prime-})}{dq^2 \Gamma(J = \rightarrow (\prime)^{+\prime-})} = \frac{1}{3} \frac{|\mathbf{F}_{\psi\eta^{(\prime)}}(q^2)|^2}{q^2} \left(1 + \frac{2m_\ell^2}{q^2}\right) \left(1 - \frac{4m_\ell^2}{q^2}\right)^{\frac{1}{2}} \frac{3}{2} \frac{(M^2; m^2; q^2)}{(M^2 - m^2)^3}; \quad (38)$$

where  $\mathbf{F}_{\psi\eta^{(\prime)}}(q^2) \equiv \mathbf{f}_{\psi\eta^{(\prime)}}(q^2) = \mathbf{f}_{\psi\eta^{(\prime)}}(0)$  is the normalized TFF, and the normalization is  $\mathbf{F}_{\psi\eta^{(\prime)}}(0) = 1$ .

In the following numerical calculations, all the values of meson masses and full widths as well as the involved decay widths and so on are quoted from the PDG [57]. The QCD running coupling constant is adopted  $\alpha_s(M=2) = 0.34$ , which is calculated through the two-loop renormalization group equation. For the value of the radial wave function at the origin  $R_\psi(0)$ , we adopt the result of the Cornell potential model [58–60]

$$|R_\psi(0)|^2 = 1.454 \text{ GeV}^3; \quad (39)$$

For  $u$ - $d$  system, by using the FKS scheme [30], the effective decay constants  $\mathbf{f}_{\eta^{(\prime)}}^q$  are parameterized as

$$\begin{aligned} \mathbf{f}_{\eta}^{u(d)} &= \frac{\mathbf{f}_q}{\sqrt{2}} \cos \theta; & \mathbf{f}_{\eta}^s &= -\mathbf{f}_s \sin \theta; \\ \mathbf{f}_{\eta'}^{u(d)} &= \frac{\mathbf{f}_q}{\sqrt{2}} \sin \theta; & \mathbf{f}_{\eta'}^s &= \mathbf{f}_s \cos \theta; \end{aligned} \quad (40)$$

and the following definitions have been used [30, 61, 62]

$$\begin{aligned} \langle 0 | J_{\mu 5}^q(0) | q(\mathbf{p}) \rangle &= i \mathbf{f}_q \mathbf{p}_\mu; & \langle 0 | J_{\mu 5}^q(0) | s(\mathbf{p}) \rangle &= 0; \\ \langle 0 | J_{\mu 5}^s(0) | s(\mathbf{p}) \rangle &= i \mathbf{f}_s \mathbf{p}_\mu; & \langle 0 | J_{\mu 5}^s(0) | q(\mathbf{p}) \rangle &= 0; \end{aligned} \quad (41)$$

with the currents  $J_{\mu 5}^q = 1 = \sqrt{2}(\bar{u} \gamma_\mu \gamma_5 u + \bar{d} \gamma_\mu \gamma_5 d)$  and  $J_{\mu 5}^s = S \gamma_\mu \gamma_5 S$ . Here the phenomenological parameters i.e., the mixing angle  $\theta$  and the decay constants  $\mathbf{f}_{q(s)}$ , can be determined by different methods [30, 63–68]. In Table II, we list the typical three sets of values for the phenomenological parameters [63, 67]. The parameters  $\theta$ ,  $\mathbf{f}_q$  and  $\mathbf{f}_s$  in the first line are extracted from the low energy processes (LEPs)  $V \rightarrow (\prime)$ ,  $(\prime) \rightarrow V$  ( $V = \rho$ ;  $\omega$ ;  $\phi$ ) [63]. The parameters in the second line are extracted from

TFF  $F_{\gamma^* \gamma \eta}(Q^2 \rightarrow +\infty)$  [67]. Obviously, these parameters both in the first and second lines are compatible with the known FKS results [30]. While in the third line, the parameters are extracted from  $\eta'$  TFF  $F_{\gamma^* \gamma \eta'}(Q^2 \rightarrow +\infty)$  [67] which is fairly consistent with the BABAR measurements in the timelike region at  $q^2 = 112 \text{ GeV}^2$  [69].

Before stepping into our numerical analysis of the branching ratios  $\mathcal{B}(J = \rightarrow (\prime)^{+\prime-})$ , we firstly discuss the normalized TFF  $\mathbf{F}_{\psi\eta^{(\prime)}}(q^2)$ . In the experimental aspect, the dependence of the modulus square of the normalized TFF  $|\mathbf{F}_{\psi\eta^{(\prime)}}(q^2)|^2$  on the dielectron invariant mass  $m_{e^+e^-}$  was explored for the first time by the BESIII Collaboration [8]. In Fig. 6, we show our results with the three sets of the parameter values from the Table II and the experimental data from Ref. [8]. We find the modulus of the normalized TFF  $|\mathbf{F}_{\psi\eta^{(\prime)}}(q^2)|^2$  is insensitive to the three sets of the parameter values, especially in the large recoil momentum region (i.e., the small dielectron invariant mass  $m_{e^+e^-}$ ). This is because many contributions caused by the three phenomenological parameters can be expected to cancel to some extent in the normalized TFF  $\mathbf{F}_{\psi\eta^{(\prime)}}(q^2)$ . To be precise, in



TABLE II. The values of  $\phi$ ,  $f_q$  and  $f_s$  obtained with three phenomenological approaches [63, 67]

	$\phi^\circ$	$f_q/f_\pi$	$f_s/f_\pi$
LEPs [63]	$40.6 \pm 0.9$	$1.10 \pm 0.03$	$1.66 \pm 0.06$
$\eta$ TFF [67]	$40.3 \pm 1.8$	$1.06 \pm 0.01$	$1.56 \pm 0.24$
$\eta'$ TFF [67]	$33.5 \pm 0.9$	$1.09 \pm 0.02$	$0.96 \pm 0.04$

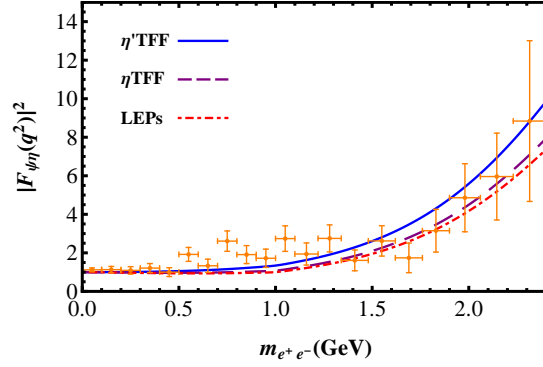


FIG. 6. The dependence of the modulus square of the normalized TFF  $|F_{\psi\eta}(q^2)|^2$  on the dielectron invariant mass  $m_{e^+e^-}$  (or,  $q^2$ ). The solid line, dashed and dash-dotted lines correspond to the three sets of parameter values, namely  $\eta'$ TFF,  $\eta$ TFF and LEPs listed in Table II, respectively. The orange dots with error bars are experimental data [8].

the hard processes, if we neglect the QED contributions, the normalized TFF  $F_{\psi\eta}(q^2)$  would be completely independent of the three phenomenological parameters. In addition, our results are roughly consistent with the experimental data. The small discrepancies in some certain regions maybe come from the resonance interaction between photons and hadrons (i.e., the VMD contributions). As an illustration, we schematically show the VMD corrections in Fig. 7, where the solid blue line (Fig. 7(a)) and the blue dots with error bars (Fig. 7(b)) are the results corresponding the set of parameter values of  $\eta'$ TFF. We find that the variation tendency of  $|F_{\psi\eta}(q^2)|^2$  is in accord with that of the experimental data when considering the VMD corrections. Interestingly enough, there are only two peaks, rather than three (corresponding the three vector mesons  $\rho$ ,  $\omega$  and  $\phi$ ) in Fig. 7(a). As we mentioned earlier, this is because the contribution of the vector meson  $\phi$  is an order of magnitude smaller than that of the vector meson  $\omega$ . Moreover, the masses of mesons  $\rho$  and  $\omega$  are very close to each other. So the low peak of the meson  $\rho$  is completely absorbed into that of the meson  $\omega$ . Furthermore, it should be noted that the VMD contributions are negligibly small in the branching ratios  $\mathcal{B}(J = \psi \rightarrow (\rho)\omega e^+e^-)$  due to the very narrow peaks (see Fig. 7(a)) and the suppression of the kinematic factors in Eq. (37) (or, Eq. (38)).

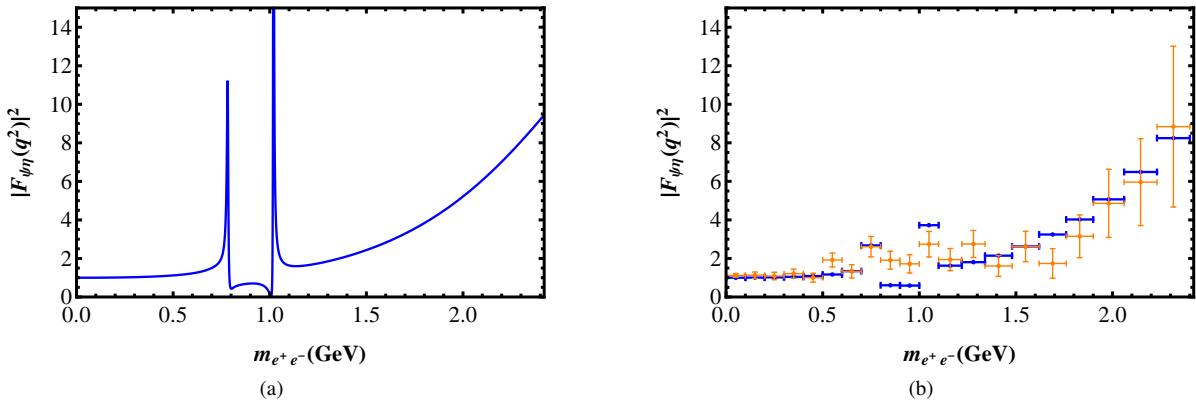


FIG. 7. The dependence of the modulus square of the normalized TFF  $|F_{\psi\eta}(q^2)|^2$  on the dielectron invariant mass  $m_{e^+e^-}$ . (a) The solid blue line shows the modulus square of the normalized TFF  $|F_{\psi\eta}(q^2)|^2$  as a function of  $m_{e^+e^-}$  (or,  $q^2$ ). (b) The blue dots with error bars are our results and the orange dots with error bars are experimental data [8].

By using the normalized TFF  $F_{\psi\eta(\rho)}(q^2)$  (i.e., the Eq. (38)), we obtain the numerical results of the branching ratios  $\mathcal{B}(J = \psi \rightarrow e^+e^-)$ ,  $\mathcal{B}(J = \psi \rightarrow \rho e^+e^-)$  and their ratio  $R_{\psi/\psi}^e = \mathcal{B}(J = \psi \rightarrow e^+e^-)/\mathcal{B}(J = \psi \rightarrow \rho e^+e^-)$  in Table III. It is clear that all

the numerical results of the branching ratios  $\mathcal{B}(J/\psi \rightarrow \eta^{(\prime)} e^+ e^-)$  and their ratio  $R_{J/\psi}^e$  are in agreement with their experimental values [8, 9], especially the ratio  $R_{J/\psi}^e$ . As discussed before, we also find that these numerical results barely depend on the three phenomenological parameters. The main reason is that the normalized TFF  $F_{\psi\eta^{(\prime)}}(q^2)$  would gloss over a lot of the dynamical information, such as the  $\eta - \eta'$  mixing. Considering the VMD corrections, we also obtain the numerical results of the branching ratios  $\mathcal{B}(J/\psi \rightarrow \eta^{(\prime)} e^+ e^-)$  and their ratio  $R_{J/\psi}^e$  with the set of the parameter values of  $\eta'$ TFF, and these results are presented in Table IV. Schematically, the differential branching ratio of  $J/\psi \rightarrow e^+ e^-$  is shown in Fig. 8 with the set of the parameter values of  $\eta'$ TFF and our results are in rough agreement with the experimental data [8]. From Tables III and IV, we find that the VMD corrections are very small in the branching ratios  $\mathcal{B}(J/\psi \rightarrow \eta^{(\prime)} e^+ e^-)$ . The main reason is that the kinematic factors suppress the contributions from VMD as well as the contributions from the small recoil momentum region. Specifically, the VMD corrections do not exceed 3% in the branching ratios  $\mathcal{B}(J/\psi \rightarrow \eta^{(\prime)} e^+ e^-)$ , especially for the branching ratio  $\mathcal{B}(J/\psi \rightarrow \eta' e^+ e^-)$ . This implies that the VMD contributions could be neglected in the EM Dalitz decay processes  $J/\psi \rightarrow \eta^{(\prime)} e^+ e^-$ .

TABLE III. The branching ratios  $\mathcal{B}(J/\psi \rightarrow \eta^{(\prime)} e^+ e^-)$  and their ratio  $R_{J/\psi}^e$  using the normalized TFF  $F_{\psi\eta^{(\prime)}}(q^2)$ .

	LEPs	$\eta$ TFF	$\eta'$ TFF	Exp. [8, 9]
$\mathcal{B}(J/\psi \rightarrow \eta e^+ e^-)$	$1.21 \times 10^{-5}$	$1.22 \times 10^{-5}$	$1.28 \times 10^{-5}$	$(1.43 \pm 0.04 \pm 0.06) \times 10^{-5}$
$\mathcal{B}(J/\psi \rightarrow \eta' e^+ e^-)$	$5.75 \times 10^{-5}$	$5.75 \times 10^{-5}$	$5.75 \times 10^{-5}$	$(6.59 \pm 0.07 \pm 0.17) \times 10^{-5}$
$R_{J/\psi}^e$	21.0%	21.2%	22.3%	$(21.7 \pm 1.2)\%$

TABLE IV. The branching ratios  $\mathcal{B}(J/\psi \rightarrow \eta^{(\prime)} e^+ e^-)$  and their ratio  $R_{J/\psi}^e$  with the VMD corrections using the normalized TFF  $F_{\psi\eta^{(\prime)}}(q^2)$ .

	$\mathcal{B}(J/\psi \rightarrow \eta e^+ e^-)$	$\mathcal{B}(J/\psi \rightarrow \eta' e^+ e^-)$	$R_{J/\psi}^e$
$\eta'$ TFF	$1.32 \times 10^{-5}$	$5.77 \times 10^{-5}$	22.9%
Exp. [8, 9]	$(1.43 \pm 0.04 \pm 0.06) \times 10^{-5}$	$(6.59 \pm 0.07 \pm 0.17) \times 10^{-5}$	$(21.7 \pm 1.2)\%$

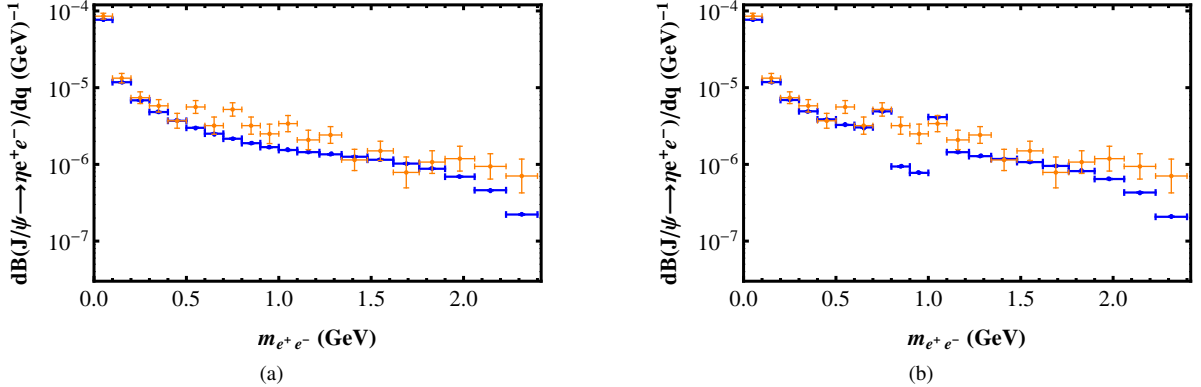


FIG. 8. The differential branching ratio of  $J/\psi \rightarrow \eta e^+ e^-$  with the set of the parameter values of  $\eta'$ TFF listed in Table II. The blue dots with error bars are our results ((a) neglecting the VMD contributions, (b) including the VMD contributions) and the orange dots with error bars are experimental data [8].

As discussed before, by using the normalized TFF  $F_{\psi\eta^{(\prime)}}(q^2)$ , some of the dynamical information would be covered up, especially for the information of  $\eta - \eta'$  mixing. Consequently, we would employ the TFF  $f_{\psi\eta^{(\prime)}}(q^2)$  (i.e., the Eq. (37)) rather than the normalized TFF  $F_{\psi\eta^{(\prime)}}(q^2)$  (i.e., the Eq. (38)) to calculate the branching ratios  $\mathcal{B}(J/\psi \rightarrow \eta^{(\prime)} e^+ e^-)$ . Our numerical results are presented in the Table V. At first glance, for the two sets of parameter values LEPs and  $\eta'$ TFF, the branching ratio  $\mathcal{B}(J/\psi \rightarrow \eta e^+ e^-)$  is estimated to be too small, which results in  $R_{J/\psi}^e$  two orders lower than the experimental value. It is interesting to note that the branching ratios  $\mathcal{B}(J/\psi \rightarrow \eta e^+ e^-)$ ,  $\mathcal{B}(J/\psi \rightarrow \eta' e^+ e^-)$  and their ratio  $R_{J/\psi}^e$  are comparable with their experimental values [8, 9], when we adopt the set of parameter values of  $\eta'$ TFF. This situation is similar to that in the radiative decay processes  $J/\psi \rightarrow \eta^{(\prime)}$  [6] and  $h_c \rightarrow \eta^{(\prime)}$  [7]. Although there are some large uncertainties included in the TFF  $f_{\psi\eta^{(\prime)}}(q^2)$  (such as the wave function of  $J/\psi$  and the QCD running coupling constant  $\alpha_s$ ), it is clear that the dynamical

information from the  $\eta - \eta'$  mixing plays an important role in the EM Dalitz decay processes  $J/\psi \rightarrow \eta^{(\prime)} e^+ e^-$ . Our results indicate that a smaller value of the mixing angle ( $\sim 34^\circ$ ) is favored in the decay processes  $J/\psi \rightarrow \eta^{(\prime)} e^+ e^-$ .

TABLE V. The branching ratios  $\mathcal{B}(J/\psi \rightarrow \eta^{(\prime)} e^+ e^-)$  and their ratio  $R_{J/\psi}^e$  using the TFF  $f_{\psi\eta^{(\prime)}}(q^2)$ .

	LEPs	$\eta$ TFF	$\eta'$ TFF	Exp. [8, 9]
$\mathcal{B}(J/\psi \rightarrow \eta e^+ e^-)$	$3.43 \times 10^{-7}$	$4.93 \times 10^{-7}$	$9.21 \times 10^{-6}$	$(1.43 \pm 0.04 \pm 0.06) \times 10^{-5}$
$\mathcal{B}(J/\psi \rightarrow \eta' e^+ e^-)$	$7.34 \times 10^{-5}$	$6.63 \times 10^{-5}$	$3.90 \times 10^{-5}$	$(6.59 \pm 0.07 \pm 0.17) \times 10^{-5}$
$R_{J/\psi}^e$	0.5%	0.7%	23.6%	$(21.7 \pm 1.2)\%$

In general, one can expect that the prediction of a ratio is more reliable, since many uncertainties from the numerator and denominator of the ratio are usually cut down to a large extent. Hence we can reliably extract the phenomenological parameters of  $\eta - \eta'$  mixing by using the ratio  $R_{J/\psi}^e$ . To proceed, along very similar lines as Refs. [6, 7], we present a determination of the three phenomenological parameters by the ratio  $R_{J/\psi}^e$

$$R_{J/\psi}^e = \frac{\int dq \frac{|f_{\psi\eta}(q)|^2}{q} \left(1 + \frac{2m_e^2}{q^2}\right) \left(1 - \frac{4m_e^2}{q^2}\right)^{\frac{1}{2}} \frac{3}{2} (M^2; m_{\eta'}^2; q^2)}{\int dq \frac{|f_{\psi\eta'}(q^2)|^2}{q} \left(1 + \frac{2m_e^2}{q^2}\right) \left(1 - \frac{4m_e^2}{q^2}\right)^{\frac{1}{2}} \frac{3}{2} (M^2; m_{\eta'}^2; q^2)} \quad (42)$$

(here the integration variable  $q$  is the dielectron invariant mass  $m_{e^+e^-}$ ), as well as the decay widths

$$\Gamma(\eta \rightarrow \gamma\gamma) = \frac{2m_{\eta}^3}{288} \left( \frac{5}{\bar{f}_q} \cos^2 - \frac{\sqrt{2}}{\bar{f}_s} \sin^2 \right)^2 \quad (43)$$

and

$$\Gamma(\eta' \rightarrow \gamma\gamma) = \frac{2m_{\eta'}^3}{288} \left( \frac{5}{\bar{f}_q} \sin^2 + \frac{\sqrt{2}}{\bar{f}_s} \cos^2 \right)^2 : \quad (44)$$

Then comparing the experimental values [8, 9, 57, 70]

$$R_{J/\psi}^{e\text{exp}} = (21.7 \pm 1.2)\%; \quad \Gamma^{\text{exp}}(\eta \rightarrow \gamma\gamma) = 0.516(18) \text{ KeV}; \quad \Gamma^{\text{exp}}(\eta' \rightarrow \gamma\gamma) = 4.36(14) \text{ KeV} \quad (45)$$

with the theoretical predictions shown in Eqs. (42), (43) and (44), we obtain the three phenomenological parameters

$$\bar{f}_q = (1.09 \pm 0.01)\bar{f}_{\pi}; \quad \bar{f}_s = (0.98 \pm 0.03)\bar{f}_{\pi}; \quad \phi = 34.0^\circ \pm 0.6^\circ \quad (46)$$

Schematically, we show the dependence of the ratio  $R_{J/\psi}^e$  on the mixing angle  $\phi$  in Fig. 9.

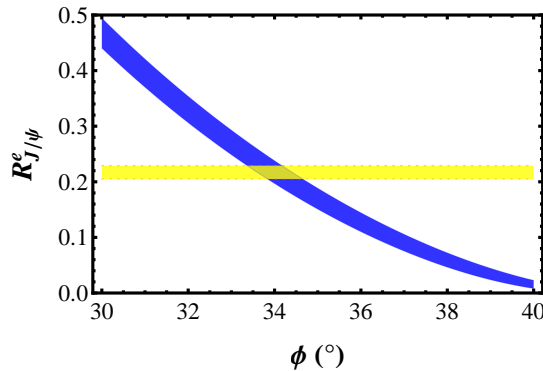


FIG. 9. The dependence of the ratio  $R_{J/\psi}^e$  on the mixing angle  $\phi$ . The blue band is our calculated results with the uncertainties from the  $\Gamma^{\text{exp}}(\eta^{(\prime)} \rightarrow \gamma\gamma)$ . The yellow band denotes the experimental value of  $R_{J/\psi}^e$  with  $1\sigma$  uncertainty.

It shows that our results of the three phenomenological parameters ( $\phi$ ,  $\bar{f}_q$  and  $\bar{f}_s$ ) are in good accord with the  $\eta'$ TFF results [67], but in clear disagreement the LEPs results [63] and the  $\eta$ TFF results [67]. In addition, the present results are consistent

with our previous determinations [6, 7], which were extracted from the ratios  $R_{J/\psi}$  and  $R_{h_c}$  in the framework of pQCD. The discrepancy in the determinations of the phenomenological parameters [6, 7, 30, 63, 67] may indicate an incomplete understanding of  $\rho - \rho'$  mixing scheme. As the  $\rho - \rho'$  mixing [71, 72], the  $\rho - \rho'$  mixing may also be an energy-dependent mixing. No matter what it is, the  $\rho - \rho'$  mixing is worthy of a further investigation. And it is worth pointing out that these Dalitz decay processes  $J = \rho \rightarrow (\rho)'+\rho'^-$  would provide a good platform to study the issue of  $\rho - \rho'$  mixing.

Using our results of the three phenomenological parameters in Eq. (46), the branching ratios  $\mathcal{B}(J = \rho \rightarrow \rho^+ \rho^-)$ ,  $\mathcal{B}(J = \rho \rightarrow \rho'^+ \rho'^-)$  and their ratio  $R_{J/\psi}^\mu = \mathcal{B}(J = \rho \rightarrow \rho^+ \rho^-) / \mathcal{B}(J = \rho \rightarrow \rho'^+ \rho'^-)$  can be predicted. Substituting the experimental values  $\Gamma^{exp}(J = \rho \rightarrow (\rho)')$  [57] into Eq. (38), we predict

$$\mathcal{B}(J = \rho \rightarrow \rho^+ \rho^-) = 3.64 \times 10^{-6}; \quad \mathcal{B}(J = \rho \rightarrow \rho'^+ \rho'^-) = 1.52 \times 10^{-5}; \quad R_{J/\psi}^\mu = 23.9\%; \quad (47)$$

where the uncertainties (we do not present) come mainly from  $\Gamma^{exp}(J = \rho \rightarrow (\rho)')$  [57], and the full uncertainties are expected to be less than 5%. As we have already mentioned, it is because most part of uncertainties caused by the TFF  $f_{\psi\eta^{(\rho)}}(q^2)$  can be removed by the normalized TFF  $F_{\psi\eta^{(\rho)}}(q^2)$  in Eq. (38).

#### IV. SUMMARY

In this work, we present a complete pQCD analysis of the EM Dalitz decays  $J = \rho \rightarrow (\rho)'+\rho'^-$  for the first time. In the large recoil momentum region, these decay processes are studied in detail with the pQCD approach. The bound state properties of  $J = \rho$  are parameterized by its B-S wave function, while  $(\rho)'$  are described by their light-cone DAs due to the large recoil momentum. Then the involved one-loop integrals are carried out analytically. Interestingly enough, we find that the TFFs  $f_{\psi\eta^{(\rho)}}(q^2)$  with small  $q^2$  are insensitive to the light quark masses and the shapes of the  $(\rho)'$  DAs, which are in line with the conclusion given in our previous work [6]. In addition, the soft contributions from the small recoil momentum region and the VMD corrections have also been taken into account, and the VMD corrections are negligible in the branching ratios  $\mathcal{B}(J = \rho \rightarrow (\rho)'+\rho'^-)$ . Furthermore, by using the ratio  $R_{J/\psi}^e$  and the decay widths  $\Gamma((\rho) \rightarrow \rho)$  as well as their experimental values, we obtain the phenomenological parameters of  $\rho - \rho'$  mixing, i.e.,  $f_q = (1.09 \pm 0.01)f_\pi$ ,  $f_s = (0.98 \pm 0.03)f_\pi$  and  $\theta = 34.0^\circ \pm 0.6^\circ$ , which are fairly consistent with the set of parameter values of  $\rho - \rho'$  TFF in Table II. Besides, the values of the phenomenological parameters obtained in this work are accord with our previous results extracted from the ratios  $R_{J/\psi}$  ( $R_{h_c}$ ) in the decay processes  $J = (\rho) \rightarrow (\rho)'$  [6, 7]. This may imply that a smaller value of the mixing angle ( $\sim 34^\circ$ ) is favored in charmonium physics.

With the extracted phenomenological parameters  $f_q$ ,  $f_s$  and  $\theta$ , we predict the branching ratios  $\mathcal{B}(J = \rho \rightarrow \rho^+ \rho^-) = 3.64 \times 10^{-6}$ ,  $\mathcal{B}(J = \rho \rightarrow \rho'^+ \rho'^-) = 1.52 \times 10^{-5}$  and their ratio  $R_{J/\psi}^\mu = 23.9\%$ . Because of the similar dynamics properties, the approach adopted in this work can also be applied to other Dalitz decays of charmonia, such as  $h_c \rightarrow (\rho)'+\rho'^-$  and  $(2S) \rightarrow (\rho)'+\rho'^-$ , which provide good ground for studying the issue of  $\rho - \rho'$  mixing and are worthy of a further investigation in both experiment and theory.

#### ACKNOWLEDGMENTS

This work is supported by the National Natural Science Foundation of China under Grant Nos. 11675061, 11775092 and 11435003.

- 
- [1] J. P. Ma, Phys. Rev. **D65**, 097506 (2002), hep-ph/0202256.
- [2] Y.-D. Yang (2004), hep-ph/0404018.
- [3] G. Li, T. Li, X.-Q. Li, W.-G. Ma, and S.-M. Zhao, Nucl. Phys. **B727**, 301 (2005), hep-ph/0505158.
- [4] Y.-J. Gao, Y.-J. Zhang, and K.-T. Chao, Chin. Phys. Lett. **23**, 2376 (2006).
- [5] B. A. Li, Phys. Rev. **D77**, 097502 (2008), 0712.4246.
- [6] J.-K. He and Y.-D. Yang, Nucl. Phys. **B943**, 114627 (2019), 1903.11430.
- [7] C.-J. Fan and J.-K. He (2019), 1906.07353.
- [8] M. Ablikim et al. (BESIII), Phys. Rev. **D99**, 012006 (2019), 1810.03091.
- [9] M. Ablikim et al. (BESIII), Phys. Rev. **D99**, 012013 (2019), 1809.00635.
- [10] M. N. Achasov et al., Phys. Lett. **B504**, 275 (2001).
- [11] R. R. Akhmetshin et al. (CMD-2), Phys. Lett. **B613**, 29 (2005), hep-ex/0502024.
- [12] R. Arnaldi et al. (NA60), Phys. Lett. **B677**, 260 (2009), 0902.2547.
- [13] D. Babusci et al. (KLOE-2), Phys. Lett. **B742**, 1 (2015), 1409.4582.
- [14] A. Anastasi et al. (KLOE-2), Phys. Lett. **B757**, 362 (2016), 1601.06565.
- [15] P. Adlarson et al., Phys. Rev. **C95**, 035208 (2017), 1609.04503.
- [16] L. G. Landsberg, Phys. Rept. **128**, 301 (1985).
- [17] M. Reece and L.-T. Wang, JHEP **07**, 051 (2009), 0904.1743.
- [18] T. Branz, A. Faessler, T. Gutsche, M. A. Ivanov, J. G. Korner, and V. E. Lyubovitskij, Phys. Rev. **D81**, 034010 (2010), 0912.3710.
- [19] C. Terschlusen and S. Leupold, Phys. Lett. **B691**, 191 (2010), 1003.1030.
- [20] C. Terschlusen and S. Leupold, Prog. Part. Nucl. Phys. **67**, 401 (2012), 1111.4907.
- [21] S. P. Schneider, B. Kubis, and F. Niecknig, Phys. Rev. **D86**, 054013 (2012), 1206.3098.
- [22] J. Fu, H.-B. Li, X. Qin, and M.-Z. Yang, Mod. Phys. Lett. **A27**, 1250223 (2012), 1111.4055.
- [23] Y.-H. Chen, Z.-H. Guo, and B.-S. Zou, Phys. Rev. **D91**, 014010 (2015), 1411.1159.
- [24] J. Zhang, J. He, T. Zhu, S. Xu, and R. Wang, Int. J. Mod. Phys. **A34**, 1950129 (2019).
- [25] S. Okubo, Phys. Lett. **5**, 165 (1963).
- [26] J. Iizuka, Prog. Theor. Phys. Suppl. **37**, 21 (1966).
- [27] V. A. Novikov, M. A. Shifman, A. I. Vainshtein, and V. I. Zakharov, Nucl. Phys. **B165**, 55 (1980).
- [28] K.-T. Chao, Phys. Rev. **D39**, 1353 (1989).
- [29] K.-T. Chao, Nucl. Phys. **B335**, 101 (1990).
- [30] T. Feldmann, P. Kroll, and B. Stech, Phys. Rev. **D58**, 114006 (1998), hep-ph/9802409.
- [31] Q. Zhao, Phys. Lett. **B697**, 52 (2011), 1012.1165.
- [32] J. H. Kühn, J. Kaplan, and E. G. O. Safiani, Nucl. Phys. **B157**, 125 (1979).
- [33] B. Guberina and J. H. Kühn, Lett. Nuovo Cim. **32**, 295 (1981).
- [34] J. G. Körner, J. H. Kühn, M. Krammer, and H. Schneider, Nucl. Phys. **B229**, 115 (1983).
- [35] B. Guberina, J. H. Kühn, R. D. Peccei, and R. Rückl, Nucl. Phys. **B174**, 317 (1980).
- [36] R. Barbieri, M. Caffo, and E. Remiddi, Nucl. Phys. **B162**, 220 (1980).
- [37] V. L. Chernyak and A. R. Zhitnitsky, Phys. Rept. **112**, 173 (1984).
- [38] A. Ali and A. Ya. Parkhomenko, Eur. Phys. J. **C30**, 367 (2003), hep-ph/0307092.
- [39] P. Ball and G. W. Jones, JHEP **08**, 025 (2007), 0706.3628.
- [40] T. Muta and M.-Z. Yang, Phys. Rev. **D61**, 054007 (2000), hep-ph/9909484.
- [41] M.-Z. Yang and Y.-D. Yang, Nucl. Phys. **B609**, 469 (2001), hep-ph/0012208.
- [42] A. Ali and Ya. Parkhomenko, Phys. Rev. **D65**, 074020 (2002), hep-ph/0012212.
- [43] S. S. Agaev, V. M. Braun, N. Offen, F. A. Porkert, and A. Schäfer, Phys. Rev. **D90**, 074019 (2014), 1409.4311.
- [44] G. 't Hooft and M. J. G. Veltman, Nucl. Phys. **B153**, 365 (1979).
- [45] A. Denner, U. Nierste, and R. Scharf, Nucl. Phys. **B367**, 637 (1991).
- [46] A. Denner, Fortsch. Phys. **41**, 307 (1993), 0709.1075.
- [47] H. H. Patel, Comput. Phys. Commun. **197**, 276 (2015), 1503.01469.
- [48] H. H. Patel, Comput. Phys. Commun. **218**, 66 (2017), 1612.00009.
- [49] P. Kroll and K. Passek-Kumerički, Phys. Rev. **D67**, 054017 (2003), hep-ph/0210045.
- [50] S. Alte, M. König, and M. Neubert, JHEP **02**, 162 (2016), 1512.09135.
- [51] M. Krammer, Phys. Lett. **B74**, 361 (1978).
- [52] A. Billoire, R. Lacaze, A. Morel, and H. Navelet, Phys. Lett. **B80**, 381 (1979).
- [53] Q. Zhao, G. Li, and C.-H. Chang, Phys. Lett. **B645**, 173 (2007), hep-ph/0610223.
- [54] G. W. Intemann, Phys. Rev. **D27**, 2755 (1983).
- [55] P. Lichard, Phys. Rev. **D83**, 037503 (2011), 1012.5634.
- [56] T. H. Bauer, R. D. Spital, D. R. Yennie, and F. M. Pipkin, Rev. Mod. Phys. **50**, 261 (1978), [Erratum: Rev. Mod. Phys.51,407(1979)].
- [57] M. Tanabashi et al. (Particle Data Group), Phys. Rev. **D98**, 030001 (2018).
- [58] E. Eichten, K. Gottfried, T. Kinoshita, K. D. Lane, and T.-M. Yan, Phys. Rev. **D17**, 3090 (1978), [Erratum: Phys. Rev.D21,313(1980)].
- [59] E. Eichten, K. Gottfried, T. Kinoshita, K. D. Lane, and T.-M. Yan, Phys. Rev. **D21**, 203 (1980).
- [60] E. J. Eichten and C. Quigg, Phys. Rev. **D52**, 1726 (1995), hep-ph/9503356.
- [61] T. Feldmann, P. Kroll, and B. Stech, Phys. Lett. **B449**, 339 (1999), hep-ph/9812269.

- [62] T. Feldmann, *Int. J. Mod. Phys. A* **15**, 159 (2000), hep-ph/9907491.
- [63] R. Escribano and J.-M. Frère, *JHEP* **06**, 029 (2005), hep-ph/0501072.
- [64] T. Huang and X.-G. Wu, *Eur. Phys. J.* **C50**, 771 (2007), hep-ph/0612007.
- [65] E. B. Gregory, A. C. Irving, C. M. Richards, and C. McNeile (UKQCD), *Phys. Rev.* **D86**, 014504 (2012), 1112.4384.
- [66] F.-G. Cao, *Phys. Rev.* **D85**, 057501 (2012), 1202.6075.
- [67] R. Escribano, P. Masjuan, and P. Sanchez-Puertas, *Phys. Rev.* **D89**, 034014 (2014), 1307.2061.
- [68] K. Ottnad and C. Urbach (ETM), *Phys. Rev.* **D97**, 054508 (2018), 1710.07986.
- [69] B. Aubert et al. (BaBar), *Phys. Rev.* **D74**, 012002 (2006), hep-ex/0605018.
- [70] D. Babusci et al. (KLOE-2), *JHEP* **01**, 119 (2013), 1211.1845.
- [71] M. Benayoun, P. David, L. DelBuono, O. Leitner, and H. B. O'Connell, *Eur. Phys. J.* **C55**, 199 (2008), 0711.4482.
- [72] M. Gronau and J. L. Rosner, *Phys. Lett.* **B666**, 185 (2008), 0806.3584.